LIGHT-HARVESTING USING METALLIC INTERDIGITATED STRUCTURES MODIFIED WITH Au SPUTTERED GRAPHENE

A. Radoi[1], M. Dragoman[1], A. Cismaru[1], G. Konstantinidis[2], and D. Dragoman[3]

[1]National Institute for Research and Development in Microtechnology (IMT),
Str. Erou Iancu Nicolae 126A, 077190 Bucharest-Voluntari, Romania
E-mail: antonio.radio@imt.ro

[2]Foundation for Research & Technology Hellas (FORTH)
P.O. BOX 1527, Vassilika Vouton, Heraklion 711 10, Crete, Hellas, Greece

[3]Univ. Bucharest, Physics Dept., P.O. Box MG-11, 077125 Bucharest-Magurele, Romania

Abstract*–Light-harvesting structures were developed using a coplanar waveguide microfabricated on high-resistivity n-Si, the central electrode consisting of an interdigitated configuration formed by two different metals. Each structure was drop casted using an aqueous dispersion of gold sputtered graphene and was thereafter subjected to I-V investigations under light excitation from UV up to IR domains. Also, the herein described device can act as a wideband photodetector with relatively good responsivity if biased.*

Keywords: *Graphene, gold, light-harvesting*

1. INTRODUCTION

Carbonaceous based materials are extensively used in many research fields, applications ranging from electric double-layer capacitors (EDLCs) [1], energy production [2], field emission [3] and fundamental electrochemistry [4]. Carbon is a versatile element, and it has been known to be present as various allotropes including graphite, diamond and fullerene-like structures. As members of the carbon family, carbon nanotubes [5] consist of seamlessly rolled up graphene layers, while graphene is a single atom monolayer of sp^2 hybridized carbon atoms organized in a honeycomb lattice [6].

Graphene can be also defined as a gapless semiconductor, with unique electronic properties, capable of reaching 200000 cm^2/Vs in suspended graphene devices [7], while the experimentally measured conductance indicates nearly the same mobility value for holes and electrons [8].
Graphene is capable of absorbing light over a broad range of wavelengths, and its many unique properties make graphene suitable for detecting light over very large bandwidth ranges [9].

978-1-4673-0738-3/12/$31.00 © 2012 IEEE

2. MATERIALS AND METHODS

Graphene was supplied by NanoIntegris, USA (PureSheets™ QUATTRO) as a water-based dispersion (0.05 mg/mL) containing 2% (w/v) ionic surfactant. In order to remove the surfactant, a certain volume of as received graphene dispersion was mixed with isopropanol and diethyl ether (1:1:2 v/v/v); in a few minutes, suspended graphene platelets gathered at the interface, between the organic and the aqueous phase (Fig. 1). The separation of graphene platelets is ascribed to the different density and solubility of each individual components described above. Taking into account that the density of diethyl ether is 0.7133 g/cm^3, while the density of isopropanol and water is 0.7854 and 0.9982 g/cm^3 [10], respectively, the ether layer (organic phase) will be above the aqueous phase (mixture of isopropanol and water). It is also important to observe that diethyl ether has limited solubility in water, while isopropanol is miscible with water.

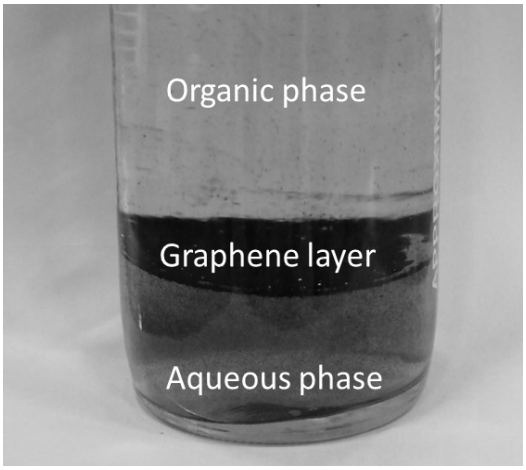

Fig. 1. Partition of graphene between organic and aqueous phase.

Little information is available about the supplied dispersion of graphene [11], but it is known to be ionic. Therefore, the graphene platelets gather at the interface of the two phases, simply by a selective affinity and float at the interface due to the large specific surface area available (2630 m^2/g) [12]. For comparison single walled carbon nanotubes possess a specific surface area in the range of 450-550 m^2/g [13]. The graphene suspension was removed and 50 mL of distilled water were added and subjected to a short sonication; again the above mentioned process was repeated five times, and in the end, the purified graphene platelets were re-suspended in distilled water (2 mL). This final dispersion was evenly spread on microscope glass slides (75×25 mm), the water was removed, and the glass slides with the deposited graphene were introduced in the sputtering chamber. Gold deposition (2 nm) was achieved using the AUTO 500 BOC Edwards, UK, while the sputter target (p > 99.99%) was supplied by MaTecK GmbH, Germany. The working conditions were: dc Ar plasma, 20 W power, 0.05 nm/s deposition rate, 99.995% gas purity, Ar flow of 3.2 cm^3/s, operating temperature 22°C, operating pressure 2×10^{-3} mbar. No post-deposition annealing treatments were performed after the gold sputtering process was terminated. SEM investigations revealed that gold islands are evenly distributed having diameters up to 20 nm in size, with a relative good coverage of the graphene platelets (Fig. 2).

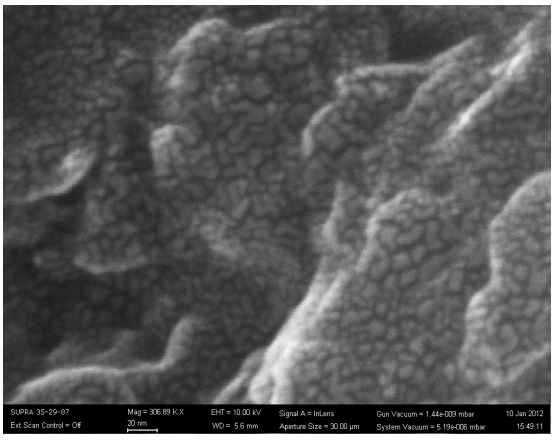

Fig. 2. SEM micrograph illustrating gold deposition on graphene.

The fractal-type pattern observed in Fig. 2 is typical for metallic sputtering depositions, depicting the collision cascade processes, which generate series of primary and higher order recoiling atoms [14].

Gold decorated graphene platelets were removed from the slides by inserting them in a Falcon™ conical tube containing 50 mL of distilled water and allowing 1 hour ultrasonic bath treatment. From this dispersion, 0.2 µL were dropped on the interdigitated electrodes, covering the entire coplanar structure, except the terminations of the electrodes where the probe tips are placed.

A standard top-down approach was adopted to produce the Au/Pt interdigitated electrode (IDT) arrays on the high-resistivity *n*-Si substrate (resistivity > 8 kΩcm). The scanning electron microscopy (SEM) micrograph revealed a coplanar configuration consisting of three electrodes: two large outer Au electrodes surrounding one central IDT electrode made of Au and Pt. On this coplanar IDT array we have deposited graphene ink decorated with gold (Fig. 3).

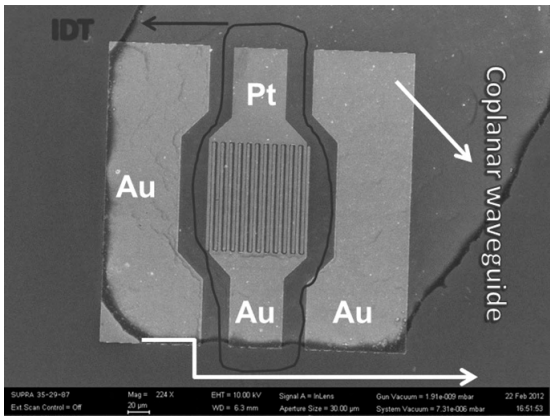

Fig. 3. SEM micrograph illustrating the configuration of the electrode.

In our experiments we used a semiconductor characterization system Keithley 4200 SCS, connected to a dark Faraday cage where the device was subjected to light excitation with: (i) a halogen lamp white light source with a tunable power and a maximum of 150 W in the visible spectrum, (ii) a UV-VIS source with 215 - 1500 nm spectral range terminated with an optical fiber, consisting of a 43 µW halogen lamp for the VIS spectral domain and a deuterium lamp with a power of 7 µW for UV, and (iii) a tungsten halogen lamp with a power of 0.5 mW as NIR source with a spectral domain of 1500 - 2500 nm. The three optical sources cover a very large spectral domain, from 215 nm to 2500 nm.

3. RESULTS AND DISCUSSIONS

Light detection and harvesting can be achieved using IDT structures, due to the generation of an electrical built-in field that contributes to the separation of the photogenerated carriers.

In our laboratory experiments we investigated the I-V behavior of the IDT structures covered with Au sputtered graphenes. We observed that under white light and IR radiation the structure was able to detect light (Fig. 4).

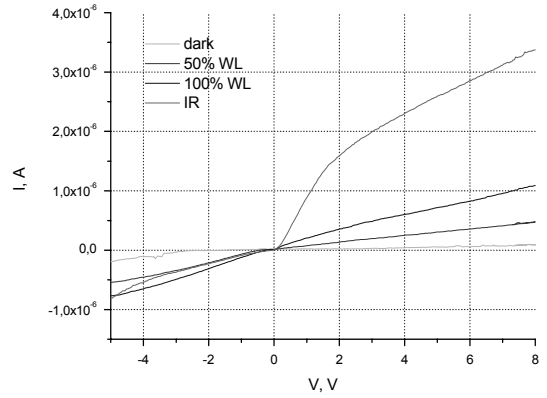

Fig. 4. I-V characteristics under white light (WL) and IR radiation.

Moreover, we investigated also the photodetection properties of such a device and we observed that in the absence of an applied potential (V = 0 V) the device is able to sense light from UV, up to VIS and IR domains (Fig. 5 (a), (b)).

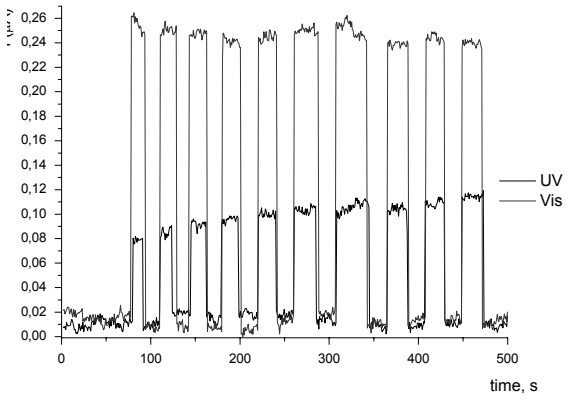

Fig. 5(a). Recordings at constant applied potential, under UV and VIS radiation.

In a subsequent series of experiments, we have connected the Pt electrode of the IDT structure with the large outer coplanar waveguide electrode made of Au. When the device was illuminated in IR (Fig. 6(b)) we obtained average values of I_{sc} = 6.6 μA and V_{oc} = 0.22 V, resulting from measurements on many devices on the same wafer (Fig. 6(b)) and estimated a filling factor of 0.66. For comparison, bare structures (without graphene) under IR radiation and dark current are illustrated in Figure 6 (a).

Finally, when both the large outer Au electrodes were contacted, the current at 0 V was very low, of few pA, despite the common believe that the harvested current must increase due to the larger collecting area.

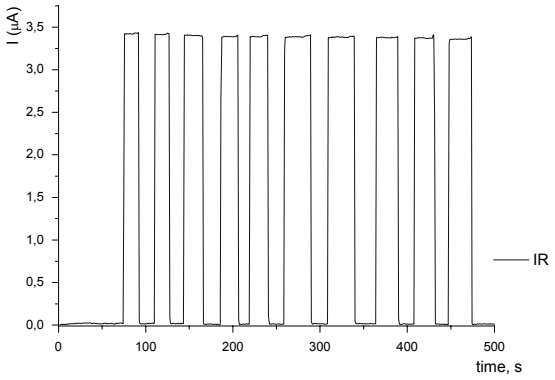

Fig. 5(b). Recordings at constant applied potential, under IR radiation.

Moreover, no harvesting effect was measured in similar devices in which the structures were patterned on 300 nm SiO_2 grown on the high resistivity *n*-Si, followed by drop casting of the graphene ink decorated with gold nanoisland on the central IDT electrode.

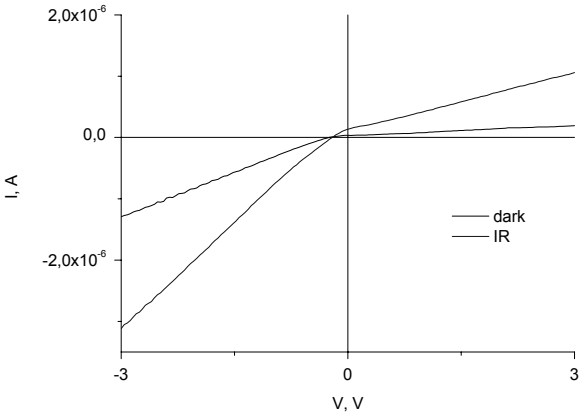

Fig. 6 (a). I-V behaviour under IR excitation of bare structures; dark current is also depicted.

We have compared Fig. 6(a) and (b) in IR because the devices provided the highest response in current. We can see from 6(a) that at 2 V the current is about 40 μA, while for the bare structure (without graphene) the current barely

reached 1 μA. So the presence of graphene decorated with metallic nanoislands increased the response about 40 times due to the additional photocarriers in the islands. This is valid also for UV and VIS. Although the IDT is covered with metallic nanoislands on graphene, there is no shortcut because: (i) graphene is a semiconductor and not a metal, even if it has no bandgap, due to its low carrier density, (ii) the nanoislands are well separated and no continuous electric path forms between electrodes.

We note that the enhancement of photogeneration/photodetection response due to the presence graphene was also very recently suggested in [15].

The experimental results can be ascribed to: (i) an electrical field perpendicular on the device assigned to Schottky contacts between *n*-Si and graphene, which prevents the recombination of photo-generated carriers by inducing charge separation and apparition of electrical dipoles inside the nanoislands; (ii) the dipoles have electrostatic images in both metallic interdigitated electrodes and the outer Au electrodes, which generate the in-plane electric fields. These opposite in-plane electric fields create a net current flow if there is a geometrical asymmetry between electrodes.

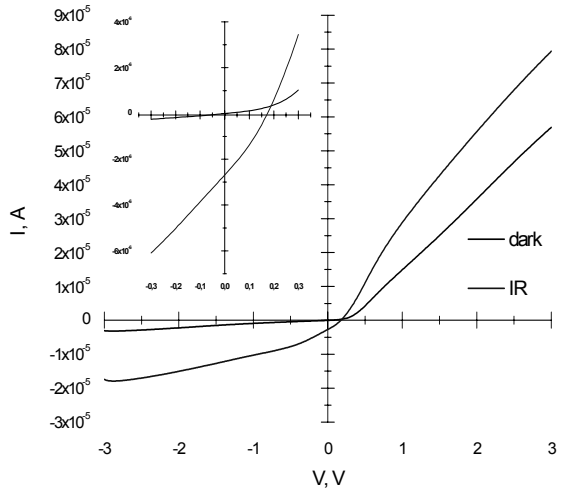

Fig. 6. (b) I-V behaviour under IR excitation; dark current is also depicted.

4. CONCLUSIONS

We demonstrated that a relatively simple device covered with graphene ink decorated with gold has potential applications in photodetection and photovoltaics. The described photodetector is a very simple device, in respect to the standard semiconductor technologies. The experimental results confirmed that the obtained photocurrent is sensitive to the excitation signal (from UV, VIS or NIR domain).

Acknowledgements–The authors Antonio Radoi and Alina Cismaru acknowledge the support of the Sectorial Operational Programme Human Resource Development (SOPHRD) under the contract number POSDRU/89/1.5/S/63700.

References

[1] Y. Zhu, H. Hu, W.C. Li and X. Zhang, J Power Sources, Cresol–formaldehyde based carbon aerogel as electrode material for electrochemical capacitor**,** 162, pp. 738–742, 2006.

[2] A. Steinfeld, Solar Thermochemical Production of Hydrogen—A Review Sol. Energy **78**, pp. 603–615, 2005.

[3] M.-Y. Teng, K.-S. Liu, H.-F. Cheng, I.-N. Lin, Electron field emission properties of carbon nanostructure synthesized by catalyst assisted solid-state growth process, Diam Relat Mater, **12**, pp. 450–455, 2003.

[4] M.D. Rubianes and G.A. Rivas, Carbon nanotubes paste electrode, Electrochem Commun **5**, pp. 689–694, 2003.

[5] P.M. Ajayan, in: M. S. Dresselhaus, G. Dresselhaus, Ph. Avouris (Eds.): Carbon Nanotubes, Topics Appl. Phys. **80**, pp. 391–425, Springer-Verlag Berlin Heidelberg 2001.

[6] A.K. Geim and K.S. Novoselov, The rise of graphene, Nature, **6**, pp. 183–191, 2007.

[7] K.I. Bolotin, K.J. Sikes, Z. Jiang, M. Klima, G. Fudenberg, J. Hone, Ultrahigh electron mobility in suspended graphene, Solid State Commun, **146**, pp. 351–355, 2008.

[8] J.C. Charlier, P.C. Eklund, J. Zhu, A.C. Ferrari, Electron and phonon properties of graphene: their relationship with carbon nanotubes, Carbon Nanotubes, **111**, pp. 673–709, 2008.

[9] F. Bonaccorso, Z. Sun, T. Hasan, A.C. Ferrari, Graphene photonics and optoelectronics, Nature photonics, **4**, pp. 611-622, 2010.

[10] http://macro.lsu.edu/HowTo/solvents/Density%20.htm

[11] http://www.nanointegris.com/en/puresheets

[12] M.D. Stoller, S. Park, Y. Zhu, J. An, R.S. Ruoff, Graphene-Based Ultracapacitors, Nano Letters, **10**, pp. 3499–3502, 2008.

[13] http://www.tedpella.com/gold_html/Nanotubes.htm

[14] P. Sigmund: Elements of Sputtering Theory. In press.

[15] J.T. Echtermeyer, P.S. Nene, M. Trushin, R.V Gorbachev, A.L. Eiden, S. Milana, Z. Sun, J. Schliemann, E. Lidorikis, K.S. Novoselov, A.C. Ferrari, Photo-thermo vs. photoelectric in metal graphene-metal-photodetectors, Graphene, Brussels, Belgium, pp. 70–71, 2012.